

**Joint COS/CARP/MSTRC Workshop
18 August 2023**

**Venue: Science Centre Lecture Theatre 1
The Chinese University of Hong Kong**

**Organized by: Centre of Optical Science (COS),
Centre for Advanced Research in Photonics (CARP), and
Materials Science and Technology Research Centre (MSTRC)**

Programme

Optical Materials and Physics

Time	Speaker and Title
9:30 – 9:50 am	Chan Pok Fung Surface Recrystallization via careful solvent design for efficient Tin Halide Perovskite Films
9:50 – 10:10 am	Liu Heng Dual-additive-driven morphology optimization for solvent-annealing-free all-small-molecule organic solar cells
10:10 – 10:30 am	Liu Yi MOF-enabled trapping of volatile organic compounds into plasmon-coupled hotspots for SERS detection
10:30 – 10:50 am	Xia Xinyue Brightening Dark Excitons in WSe ₂ Monolayer at Room Temperature with Au Nanodisk-on-Mirror Structures
10:50 – 11:10 am	Zhao Xinyi Tunable Kerker scattering in a self-coupled metasurface
11:10 – 11:30 am	Zhou Yaoqiang Two-dimensional Schottky Barrier Field-effect Transistor with Programmable Photovoltaic Performance
11:30 – 11:50 am	Ai Ruoqi Orientation-dependent interaction between the magnetic plasmons in gold nanocups and the excitons in WS ₂ monolayer and multilayer
11:50 am – 12:10 pm	He Xie Miniaturized Spectrometers Based on Bias-Tunable Photomultiplication-Type Organic Photodetectors
12:10 – 12:30 pm	Liu Rong Green-Manufactured and Recyclable Coatings for Subambient Daytime Radiative Cooling
12:30 – 12:50 pm	Zhou Nansen Transmission Matrix-based High Sensitivity Quantitative Phase Profilometry for Accurate and Fast Thickness Mapping of 2D Materials

Optical Devices and Instrumentation

Time	Speaker and Title
2:00 – 2:20 pm	Chen Shuyan Photovoltaic-Based Visible Light Communications and its Alternate-Current Dynamics
2:20 – 2:40 pm	Li Zijian All-Optical Purification of Arbitrary Spectral Waveforms via Cross-Phase Modulation Based Talbot Amplifier

2:40 – 3:00 pm	Xue Ying In-plane 1.5 μm DFB lasers on SOI for integrated photonics
3:00 – 3:20 pm	Wang Geyang A Digital Signal Processing Perspective on Enhancing Capacity and Security of Bandwidth-Limited LED/Laser Communication Systems
3:20 – 3:40 pm	Wang Yintao Random Access Particle Tracking
3:40 – 4:00 pm	Xu Chao Ultrahigh-resolution Miniaturized Visible-light Optical Coherence Tomography Endoscopy
4:00 – 4:20 pm	Xu Tengji A power efficient and high precision micro-ring weight bank sparsity resolving the thermal challenges
4:20 – 4:40 pm	Yan Yue On chip photothermal spectroscopy for gas detection
4:40 – 5:00 pm	Tinghua Zhang A steerable OCT endoscope using pneumatic motor
5:00 – 5:20 pm	Zhu Zhiwei Scan-less phase imaging based on a single-cavity dual-comb laser with spatiotemporal encoding
5:20 – 5:50 pm	Liu Peng In vivo ultrahigh-resolution imaging in airways using 800-nm OCT endoscopy
5:50 – 6:10 pm	Luo Mingcheng Optical Metasurfaces for Medical Image Classification

Surface Recrystallization via careful solvent design for efficient Tin Halide Perovskite Films

Pok Fung Chan¹, Minchao Qin¹, Chun-Jen Su², Liping Ye³, Xuezhou Wang⁴, Yunfan Wang⁵, Xin Guan³, To Ngai³, Sai Wing Tsang⁵, Ni Zhao⁴, Qian Miao³, and Xinhui Lu^{1,*}

¹Department of Physics, The Chinese University of Hong Kong, New Territories 999077, Hong Kong SAR, China

²National Synchrotron Radiation Research Center, Hsinchu Science Park, Hsinchu 30076, Taiwan

³Department of Chemistry, The Chinese University of Hong Kong, New Territories 999077, Hong Kong SAR, China

⁴Department of Electronic Engineering, The Chinese University of Hong Kong, New Territories 999077, Hong Kong SAR, China

⁵Department of Materials Science and Engineering, City University of Hong Kong, Kowloon Tong 999077, Hong Kong, China

*E-mail: xinhui.lu@cuhk.edu.hk

Abstract: The surface of tin-based perovskite film was recrystallized by *iso*-BAI in a mixture of methyl butanol and chlorobenzene to passivate the surface and keep the bulk film intact. The corresponding solar cell devices reached a power conversion efficiency of 14.2%.

Tin-based perovskite solar cells (PSC) are becoming promising substitutes for their toxic lead counterparts. However, tin-based PSCs are prone to oxidation and thus still exhibit inferior device performance[1]. Owing to the different chemical properties of lead (II) and tin (II) ions, the mechanisms for reliable film preparation processes are still under exploration. Herein, we propose a surface treatment to modify the surface of tin-based perovskite using a commonly used ligand, iso-butylammonium iodide (*iso*-BAI). We demonstrate that the mechanism of the surface treatment in tin-based perovskite originates from the recrystallization of the surface due to the higher solubility of tin-based perovskite in common solvent, which is different from the lead counterparts. With a carefully designed solvent composition, we successfully modify the perovskite surface (Fig. 1e,f) while keeping the bulk intact. X-ray diffraction measurements reveal that the perovskite surface dissolves and re-crystallizes with the guidance of *iso*-BAI. The resultant films exhibit enhanced surface crystallinity (Fig. 1a,b), released microstrain (Fig. 1c), reduced surface defects, and improved charge transport. With the surface treatment, the power conversion efficiency of the FASnI₃ perovskite solar cells increases from 11.8% to 14.2%, which is close to the current record. This work first distinguishes the mechanism of surface treatments in tin-based perovskite from that of the lead counterpart, which is crucial for designing tailor-made strategies for fabricating tin-based PSCs.

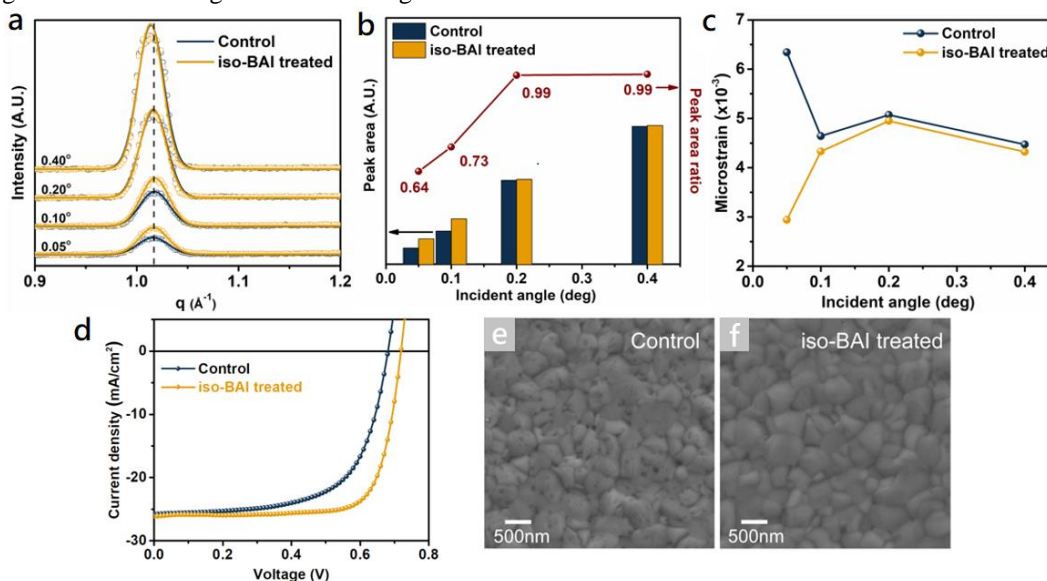


Figure 1. (a) GIWAXS intensity profile, (b) (100) peak intensity ratio, and (c) Estimated microstrain of the control and the *iso*-BAI treated film. (d) JV curve of the solar cell devices. SEM image of (e) the control and (f) *iso*-BAI treated film

References

1. Lanzetta, L., et al., Nat Commun, 2021. **12**(1): p. 2853.

Dual-additive-driven morphology optimization for solvent-annealing-free all-small-molecule organic solar cells

Heng Liu, Yuang Fu, Xinhui Lu*

Department of Physics, The Chinese University of Hong Kong, New Territories 999077, Hong Kong SAR, China

*Corresponding author. E-mail: xinhui.lu@cuhk.edu.hk

Abstract: This study developed a dual-additive-driven morphology optimization method for All-small-molecule organic solar cells (ASM-OSCs). After the synergistic morphology tuning, the optimized device delivered a PCE as high as 15.2%.

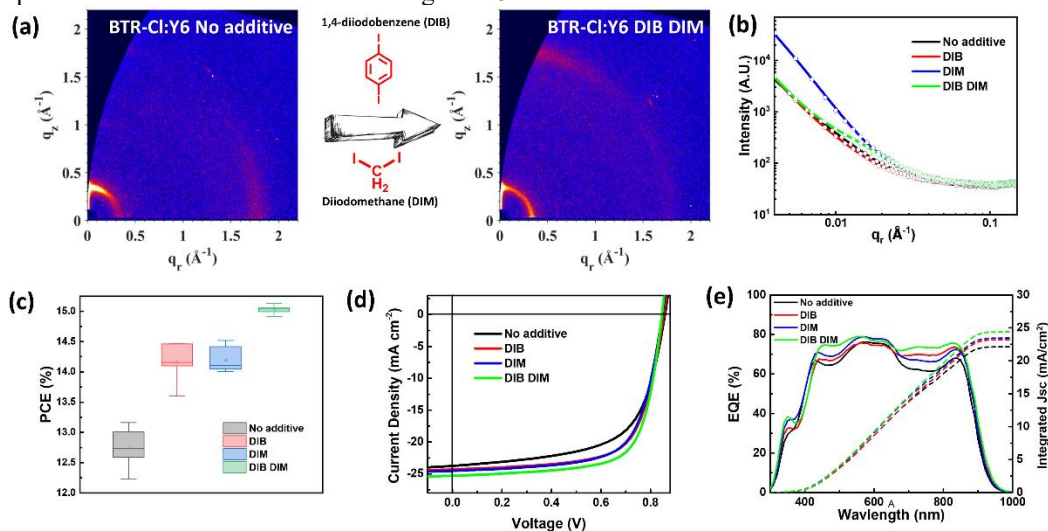


Figure 1. a) 2D GIWAXS patterns of BTR-Cl/Y6 and BTR-Cl/Y6/DIB/DIM. b) GISAXS profiles and best fittings results along the in-plane direction. c) Statistical histograms of PCE. d) J–V curves. e) EQE response and integrated J_{sc} of best-performing devices.

All-small-molecule organic solar cells (ASM-OSCs), which consist of small-molecule donor and acceptors, have recently been studied extensively to eliminate the batch-to-batch variation from polymer-based donor or acceptor. On the other hand, the control of their active layer morphology is more challenging. In this study, we combined one solid additive 1,4-diiodobenzene (DIB) and one liquid additive - diiodomethane (DIM) and the combination can change the orientation of BTR-Cl from edge-on to face-on in the blend film which is beneficial for charge transport¹. (Fig 1a) The optimized active layer with suitable domain size and favourable molecular packing benefits from charge recombination, charge extraction and more efficient charge transport². (Fig 1b) As a result, a PCE of 15.2% has been realized in ASM-OSCs without SVA treatment. (Fig 1c and d) The dual additive approach illustrated in this work offers a promising route to regulate film morphology toward highly efficient ASM-OSCs.

References

1. S. Chen, J. Ye, Q. Yang, J. Oh, D. Hu, K. Yang, G. O. Odunmbaku, F. Li, Q. Yu and Z. Kan, *J. Mater. Chem. A*, 2021, **9**, 2857-2863.
2. J. Teixeira, *J. Appl. Crystallogr.*, 1988, **21**, 781-785.

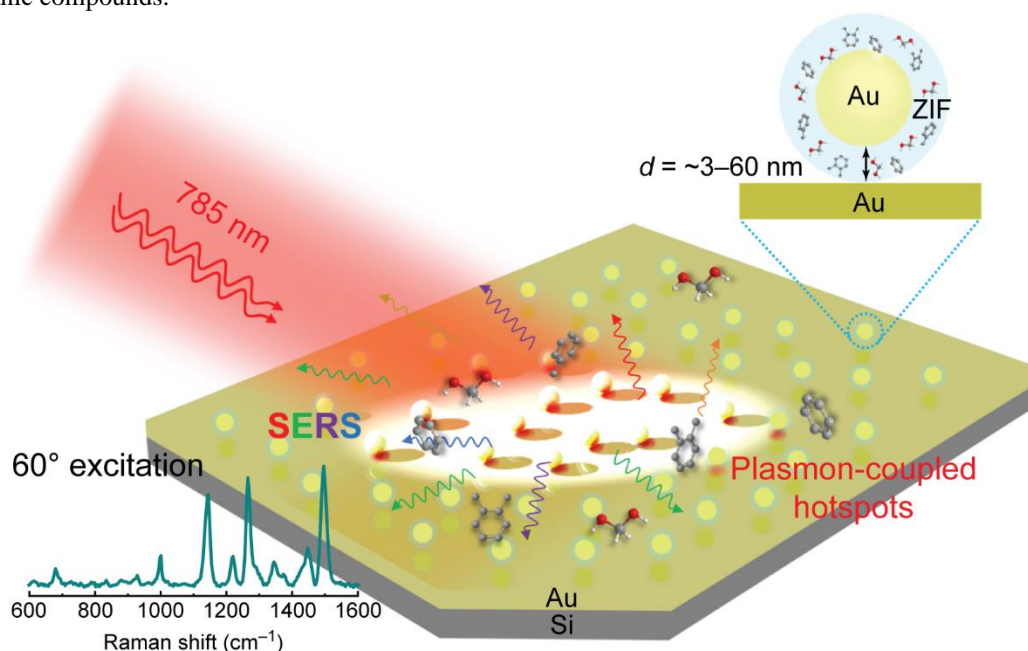
MOF-enabled trapping of volatile organic compounds into plasmon-coupled hotspots for SERS detection

Yi Liu, Jianfang Wang*

Department of Physics, The Chinese University of Hong Kong, Shatin, Hong Kong SAR 999077, China.

*Email: jfwang@phy.cuhk.edu.hk

Abstract: Utilizing hotspots within plasmonic nanogaps is a promising approach to build ultrasensitive surface-enhanced Raman scattering (SERS) substrates. The SERS signals of chemical molecules located in the nanogaps can be greatly amplified by up to 10^{18} -fold. Besides the enhancement of the electric field in SERS substrates, the improvement of molecule concentrations to be detected is also an effective approach to obtain outstanding SERS performance. Metal-organic frameworks (MOFs) are commonly used to absorb and concentrate molecular species. Herein we combine these two strategies by introducing a MOF into plasmon-coupled nanogaps, which has, however, remained experimentally challenging so far. The ultrasensitive SERS substrates are achieved through the construction of particle-on-mirror structures, where Au nanocrystals are encapsulated with MOF shells and then coupled with Au films. The MOF shell, as a spacer that separates Au nanocrystals and Au films, can be regulated in thickness over a wide range, which allows the electric field enhancement, plasmon resonance wavelength, and molecular enrichment effect to be adjusted. By trapping Raman-active molecules within the MOF shell, we show that our plasmon-coupled structures exhibit superior SERS detection performance towards a range of volatile organic compounds.



Brightening Dark Excitons in WSe₂ Monolayer at Room Temperature with Au Nanodisk-on-Mirror Structures

Xinyue XIA¹, He Huang¹, Jianfang Wang^{1*}

¹Department of Physics, The Chinese University of Hong Kong, Shatin, Hong Kong SAR 999077, China. ²Department of Applied Physics, The Hong Kong Polytechnic University, Kowloon, Hong Kong SAR 999077, China.

*email: jfwang@phy.cuhk.edu.hk

Abstract:

Dark excitons in transition metal dichalcogenide (TMDC) monolayers (MLs) are promising candidates for the Bose–Einstein condensation and can be applied for quantum information processing due to their long lifetime. Such excitons involve spin-forbidden optical transitions corresponding to almost zero in-plane transition dipole moment. Their emissions therefore have been investigated under critical conditions such as cryogenic temperature and high magnetic field due to their weak interactions with light. One way to enhance the emission efficiency of dark excitons is to insert TMDC MLs into an out-of-plane electromagnetic field with which the dipole moments of dark excitons align. Here, we brighten the dark excitons of WSe₂ ML at room temperature with hybrid structures constructed by (Au nanodisk)-on-mirror nanocavities with WSe₂ MLs sandwiched in between. Highly tunable in-plane magnetic modes and out-of-plane toroidal modes are excited by precisely controlling the diameters of Au nanodisks. Both in-plane and out-of-plane plasmon modes of the (Au nanodisk)-on-mirror nanocavities give rise to a large area of the greatly confined out-of-plane electric field within the WSe₂ ML, which boosts the radiative decay rates of dark excitons through the Purcell effect. The emission intensity ratio between dark excitons and A excitons is enhanced by up to 22 times by tuning the plasmon energy to match with the dark exciton energy. Our hybrid structures therefore provide a facile strategy for brightening dark excitons at ambient conditions.

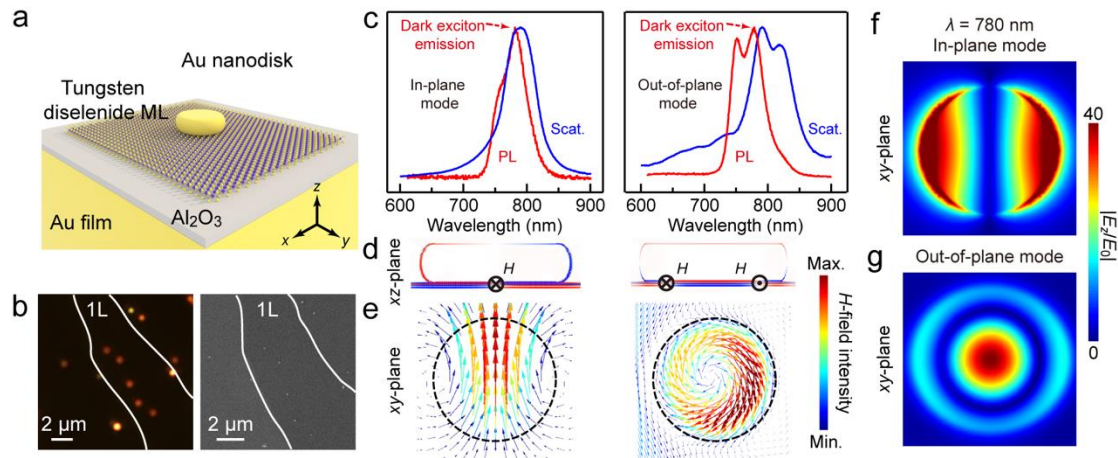


Fig. 1. (a) Schematic of a (WSe₂ ML)-sandwiched Au nanodisk-on-mirror structure. (b) Dark-field scattering (left) and corresponding SEM (right) images. (c) Photoluminescence (PL) and scattering spectra under the modulation of the in-plane (left) and out-of-plane (right) cavity modes. (d,e) Charge distribution contours and magnetic field distribution contours of the in-plane (left) and out-of-plane modes (right) at 780 nm, respectively. (f,g) Simulated z-component electric field enhancement contours.

Tunable Kerker scattering in a self-coupled metasurface

Xinyi Zhao, Fuhuan Shen, Jianbin Xu*

Department of Electronic Engineering, The Chinese University of Hong Kong, Shatin, N.T., Hong Kong SAR, P. R. China.
jbxu@ee.cuhk.edu.hk (J. B. Xu)

Abstract: The dynamical control of the directional scattering, i.e., Kerker scattering, of dielectric nanostructure by tuning the exciton-photon coupling is demonstrated. A self-coupled metasurface based on MoS₂ is experimentally fabricated, showing forward/backward (F/B) scattering ratio up to 20. Moreover, the scattering directionality can be tuned by decreasing the temperature, during which process the excitonic properties of MoS₂ are changed.

Strong coupling between electronic transition and resonant cavity mode via coherent energy transfer offers unprecedented opportunities to tailor the photoelectronic properties of constituent components. The hybrid state, also known as polariton, bridges the light and matter in a monolithic structure [1]. In this report, we demonstrate the dynamical control of the directional scattering, i.e., Kerker scattering, of dielectric nanostructure by tuning the exciton-photon coupling. We firstly theoretically prove a giant modification of scattering directionality of the dielectric metastructure engineered by the excitonic polariton (Fig. 1a) [2]. As a proof of concept, self-coupled metasurfaces based on bulk MoS₂ (schematically shown in Fig. 1b-c) are built, showing a forward/backward scattering up to 20 as well as a tunable directionality by thermally controlling the excitonic coupling to the Mie modes (Fig. 1f-h), which is of great significance. The simulated results show a decent agreement to the measured ones, with following multipole decompositions well demonstrating the behind mechanism due to the superposition of electric and magnetic dipole modes modified by excitons. Our work sheds light on controlling the light flow in the far field by coherent light-matter interaction, and opens many possibilities for active optical antennas and quantum emitters at the nanoscale.

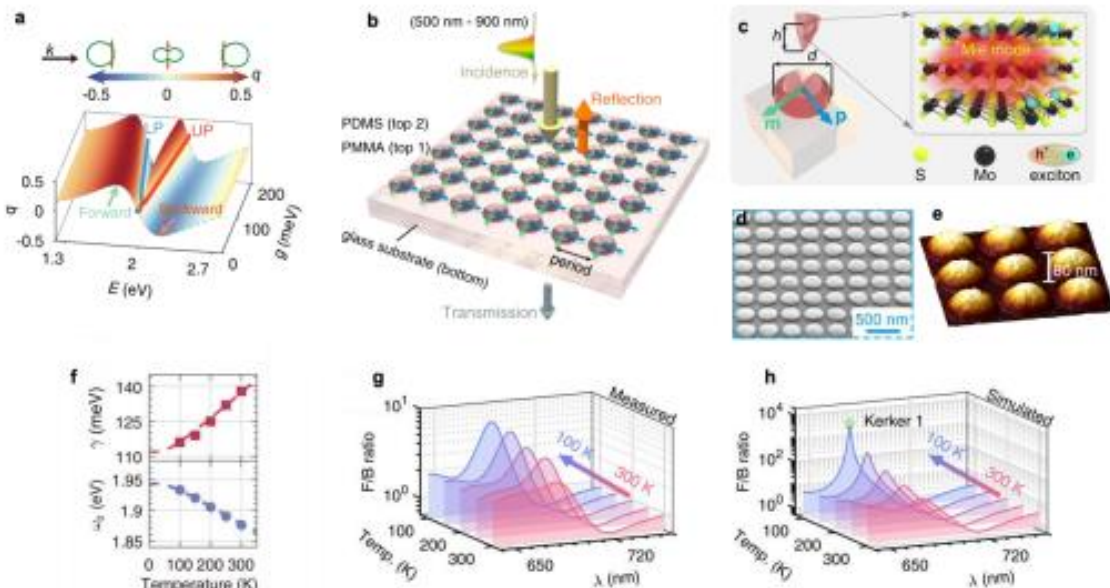


Fig. 1. Tunable Kerker scattering in a self-coupled metasurface. (a) Evolution of asymmetric factor q as a function coupling strength g . (b) Schematic image of a MoS₂ self-coupled metasurface. (c) Zoom-in image of MoS₂ disk where support both the Mie modes and excitons. (d, e) SEM (d) and AFM (e) image of the MoS₂ metasurface. (f) Temperature-dependent excitonic properties. (g, h) Measured (g) and simulated (h) temperature-dependent forward/backward ratio of the MoS₂ self-coupled metasurface.

References

- [1] Nat. Nanotechnol. 14, 679–683 (2019).
- [2] Nat Commun 13, 5597 (2022).

Two-dimensional Schottky Barrier Field-effect Transistor with Programmable Photovoltaic Performance

Yaoqiang Zhou* and Jian-Bin Xu

Department of Electronic Engineering, The Chinese University of Hong Kong
*yqzhou@link.cuhk.edu.hk

Abstract: Reconfigurable non-volatile Schottky-barrier field-effect transistor (SBFET) with semimetal WTe_2 as the self-gating bottom contact is fabricated. The programmable photovoltaic performance of the non-volatile SBFET is demonstrated, showcasing a wide range of self-powered responsivity from -50 mA/W to 290 mA/W .

Brain-inspired technology can boost edge computing as a sophisticated in-memory computing approach to overcome the von Neumann bottleneck. Similar to the flexibility and adaptability of connection in the human brain, brain-inspired electronic and photoelectronic devices can be reconfigured to execute different computational tasks. [1] Furthermore, like the memory function of synapses, the brain-inspired device can also retain information for future retrieval and processing. Emerging SBFETs exhibiting inherently ambipolar transfer characteristics in the single dopants-free semiconducting channel have been expected to establish the runtime reconfigurable in-memory architecture mimicking the brain. [2] State-of-the-art SBFETs built by 2D semiconductors and bulk metals have suffered from a strong Fermi-level pinning effect, which hinders the improvement of the design flexibility of SBFETs. To solve this problem, we proposed a vertically stacked non-volatile SBFET with semimetal WTe_2 as the self-gating bottom contact. [3] The effective barrier height offset $\Delta\Phi_B$ was programmed from $\Delta\Phi_{B-p} = 132.6 \text{ meV}$ to $\Delta\Phi_{B-n} = 109.4 \text{ meV}$ due to the interfacial charge transferring. The non-volatile SBFET can serve as a reconfigurable artificial synapse, in which the multilevel resistance states can be cooperatively controlled by encoding the incremental or decremental global gate pulses at identical voltage amplitudes with the drain bias direction. In addition, assisted with graphite as the top transparent electrode, the non-volatile SBFET provides a platform to enrich optoelectronic functionalities based on reconfigurable self-powered photovoltaic performance. By gate voltage spike-writing, the open-circuit voltage of non-volatile SBFET can be modulated from -0.1 V to 0.25 V , and the multilevel self-powered responsivity can also be programmed from -50 mA/W to 290 mA/W . These properties render non-volatile SBFET promising for new brain-inspired optoelectronics with in-memory optical sensing and real-time machine vision.

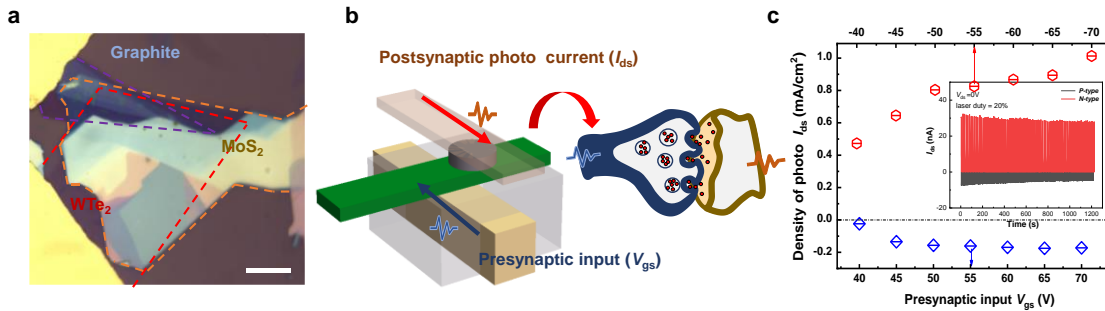


Fig. 1. Structure and programmable photo response of the vertical artificial synapse. a) Optical image of the non-volatile SBFET. b) Schematic of the SBFET synapse in which V_{gs} simulates the presynaptic input and the channel current I_{ds} is monitored as the post-synaptic current. c) Short-circuit current density programmed by the V_{gs} input spikes. The inset shows the retention properties of the bi-stable self-powered photocurrent.

References

- [1] H.-T.Zhang, T. J.Park, A. N. M. N.Islam, D. S. J.Tran, S.Manna, Q.Wang, S.Mondal, H.Yu, S.Banik, S.Cheng, H.Zhou, S.Gamage, S.Mahapatra, Y.Zhu, Y.Abate, N.Jiang, S. K. R. S.Sankaranarayanan, A.Sengupta, C.Teuscher, and S.Ramanathan, "Reconfigurable perovskite nickelate electronics for artificial intelligence," *Science*. **375**, 533–539 (2022).
- [2] Y.Zhou, L.Tong, Z.Chen, L.Tao, Y.Pang, and J.-B.Xu, "Contact-engineered reconfigurable two-dimensional Schottky junction field-effect transistor with low leakage currents," *Nat. Commun.* **14**, 4270 (2023).
- [3] Y.Zhou, L.Tong, Z.Chen, L.Tao, H.Li, Y.Pang, and J.-B.Xu, "Vertical Nonvolatile Schottky-Barrier-Field-Effect Transistor with Self-Gating Semimetal Contact," *Adv. Funct. Mater.* **n/a**, 2213254 (2023).

Orientation-dependent interaction between the magnetic plasmons in gold nanocups and the excitons in WS₂ monolayer and multilayer

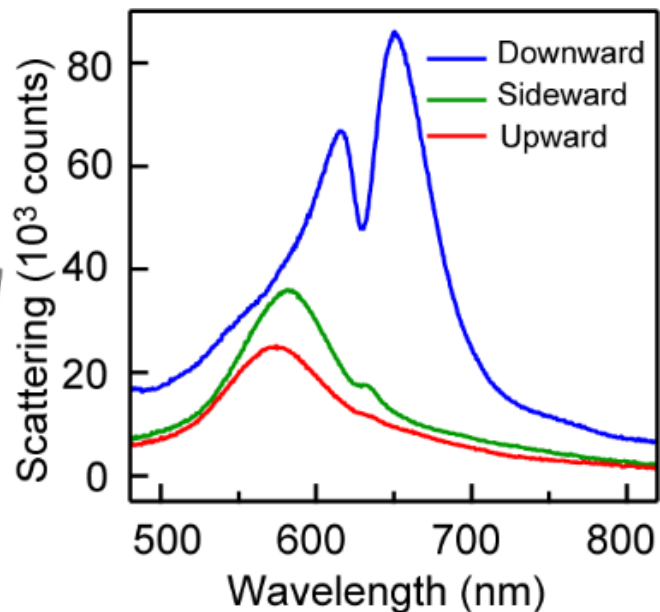
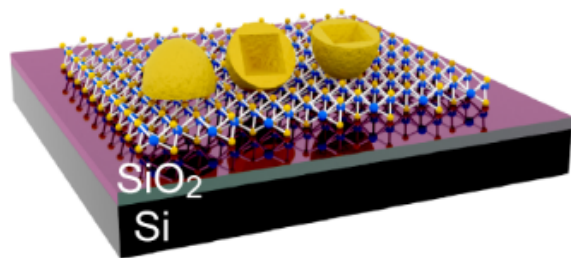
Ruoqi AI¹, Xinyue XIA¹, Jianfang Wang^{1*}

¹Department of Physics, The Chinese University of Hong Kong, Shatin, Hong Kong SAR 999077, China.

*email: jfwang@phy.cuhk.edu.hk

Abstract:

Strong coupling is essential for the investigations like threshold less lasing, single-photon switching and quantum emitter. However, Light-matter interaction is hard to realize in the free space due to the unmatched between the light wavelength and the emitter. Herein, a strong coupling between the magnetic plasmons and excitons is investigated on (Au nanocup)-on-(WS₂ monolayer/multilayer) hybrid structures. The asymmetric morphology of Au nanocups allows both electric and magnetic plasmon resonances on the individual particles. By varying the opening of Au nanocups from sideward and upward to downward orientations, resonance coupling from weak to strong is achieved, accompanied by a large split mode shown up in the dark-field scattering spectrum. Such a large split mode stems from the pronounced electric and magnetic field enhancement generated between the downward-orientated Au nanocups and the substrate. The detuning between the magnetic plasmons and the excitons in the WS₂ monolayer was modulated by varying the size of downward-orientated Au nanocups. A Rabi splitting up to 106 meV was realized at the zero detuning. Size-dependent measured scattering and simulated absorption spectra further corroborate the strong coupling in the hybrid structures. The Rabi splitting further increases in the wake of the increasing thickness of the WS₂ layer to four and keeps saturated when the WS₂ layer is up to five. Such a simple hybrid structure allows the further investigation of strong coupling-based applications in optics and optoelectronics. It also provides a facile strategy to manipulate the emissions of diverse excitons in two-dimensional transition metal dichalcogenides.



Miniaturized Spectrometers Based on Bias-Tunable Photomultiplication-Type Organic Photodetectors

Xie He, Ni Zhao*

Department of Electronic Engineering, The Chinese University of Hong Kong, Shatin, New Territories, Hong Kong SAR, China
*nzhao@ee.cuhk.edu.hk

Abstract: A miniaturized spectrometer is proposed and experimentally demonstrated based on photomultiplication-type organic photodetectors. Incident light spectra can be computationally reconstructed from the different spectral responses and measured photocurrents under different bias voltage. Broadband operation across the visible spectrum regime with <5 nm resolution was achieved within a remarkably small footprint of only 0.0004 cm².

Optical spectrometers are essential instruments for various applications, including material characterizations, medical diagnosis, food sciences, and biomedical sensing. Conventional benchtop spectrometers can achieve high performance through the use of dispersive components, long optical path lengths, and intricate movable mechanisms, which however result in their high cost and bulky size. To address the increasing demand for compact and low-cost spectrometers that can be integrated with wearable and portable system platforms, there have been great research efforts in recent years to develop device technologies for spectrometer miniaturization. Nevertheless, current solutions still face challenges such as labor-intensive and complicated device fabrication processes and reproducibility of the device performances. In this work, we propose and experimentally demonstrate a computationally reconstructive spectrometer, which is achieved through in-situ photogain modulation controlled by the electric field induced redistribution of trapped photocarriers in a photomultiplication-type organic photodetector (PM-OPD). Novel top contact electrodes with high transparency and low work function were developed, enabling optical spacer integration for spectral and spatial light manipulation. As a result, broadband operation across the visible spectrum regime (400~760 nm) with <5 nm resolution was demonstrated within a remarkably small footprint of only 0.0004 cm². The fabrication process is predominantly solution-based, ensuring cost-effectiveness and scalability. This work is the first to demonstrate a PM-OPD utilizing dynamic modulation of photocarriers, expanding the applications of organic optoelectronic devices and providing a promising device solution for hyperspectral imaging (HSI) applications.

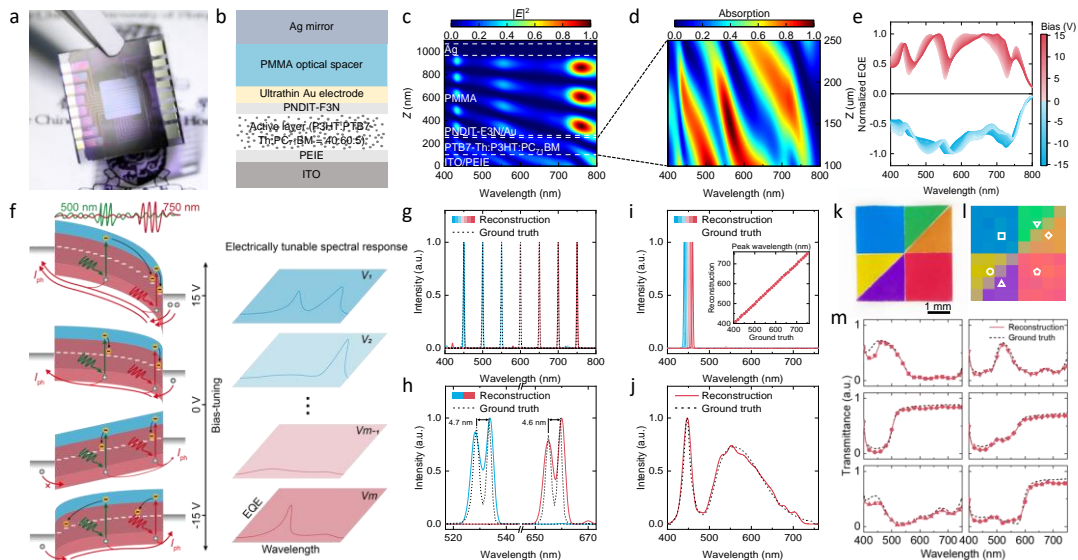


Fig. 1. (a) Photograph and (b) schematic illustration of the device. (c) Simulated electric field and (d) absorption profile. (e) Normalized EQE spectrum under $-15\text{V}\sim+15\text{V}$ bias voltage. (f) Schematic illustration of the bias-modulation effect. (g-j) Demonstration of spectrum reconstruction. (k-m) Demonstration of hyperspectral imaging. (k) Photograph and (l) reconstructed image of a color filter patch. (m) Transmittance spectrum of selected pixels.

Green-Manufactured and Recyclable Coatings for Subambient Daytime Radiative Cooling

Rong Liu and Yi Long*

Department of Electrical Engineering, The Chinese University of Hong Kong, Shatin, New Territories, Hong Kong, China
*ylong@ee.cuhk.edu.hk

Abstract: Passive daytime radiative cooling requires materials with high solar reflectance and thermal emittance. An eco-friendly radiative cooling coating with a record solar reflectance of 98.6% and thermal emittance of 98.1% was fabricated by convenient paint-like operation.

Passive daytime radiative cooling, which reflects sunlight and simultaneously emits heat into space to cool surfaces without energy input, is a promising strategy for energy conservation [1]. Integrating radiative cooling with building systems can tremendously alleviate electrical cooling, but manufacturing high-efficient and eco-friendly coatings remains an urgent and challenging task [2]. Here, we present a simple and scale-up strategy for fabricating ultra-white coating consisting of porous ethyl cellulose matrix-random BaSO₄ nanoparticles by utilizing green solvents [Fig. 1(a),(b)]. With the synergistic effect of the ideal intrinsic properties of the materials and the strong Mie scattering of the porous structure [Fig. 1(c)], the ultra-white coating possesses a record solar reflectance of 98.6% and thermal emittance of 98.1% [Fig. 1(d),(e)], resulting in a sub-ambient temperature drops of over 2.5 °C under a solar intensity of ~920 W m⁻². Better yet, our coatings can be conveniently brushed, rolled, or sprayed onto various types of substrates, with excellent durability, self-cleaning, and cost-effectiveness, paving an attractive and viable pathway for large-scale applications in practical buildings.

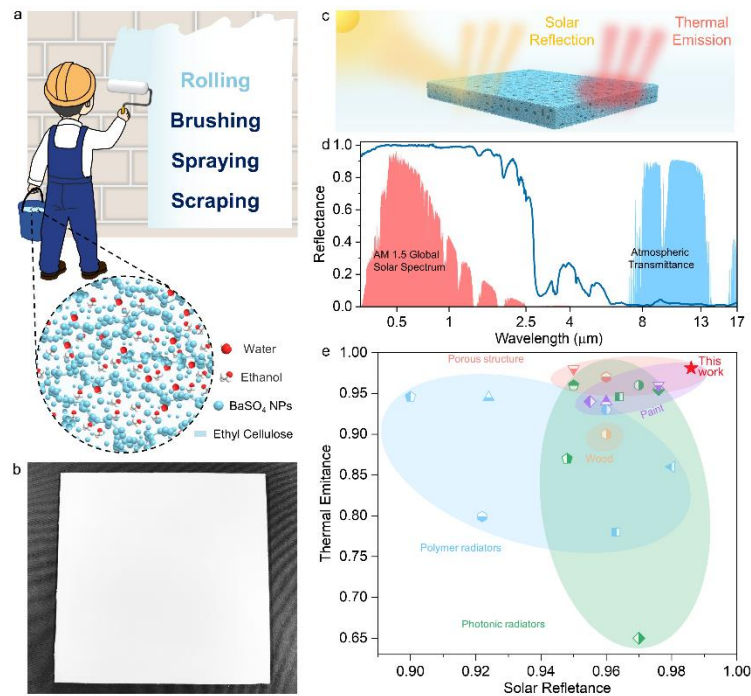


Fig. 1. Fabrication and optical properties of the ultra-white coating. (a) Schematic of the coating fabrication by different painting methods (top). The slurry includes four-component of BaSO₄ NPs (optical scatterer), ethyl cellulose (EC) (polymer binder), water (nonsolvent) and ethanol (solvent) (bottom). (b) Photo of the uniform bright white coating (10 cm × 10 cm). (c) Schematic mechanism of our coating for highly efficient daytime radiative cooling. (d) Spectral reflectance of the coating with the normalized AM1.5 global solar spectrum (shaded red) and atmospheric transmittance (shaded blue) plotted for reference. (e) Optical properties (solar reflectance and thermal emittance) comparison of reported PDRC materials.

References

- [1] A. P. Raman *et al.*, Nature **515**, 540–544 (2014); S. Wang *et al.*, Science **374**, 1501-1504 (2021).
- [2] J. Mandal *et al.*, Science **362**, 315–319 (2018); J. Mandal *et al.*, Joule **4**,1350–1356 (2020).

Transmission Matrix-based High Sensitivity Quantitative Phase Profilometry for Accurate and Fast Thickness Mapping of 2D Materials

Nansen Zhou and Renjie Zhou*

Department of Biomedical Engineering, The Chinese University of Hong Kong, Hong Kong, China

*rjzhou@cuhk.edu.hk

Abstract: The transmission matrix based quantitative phase profilometry (TM-QPP) is proposed to achieve picometer-level optical pathlength sensitivity. The accurate thickness determination with ~ 10 pm precision is demonstrated by wide-field mapping monolayer and few-layered 2D materials.

The physical properties of two-dimensional (2D) materials and related optoelectronic devices may drastically vary with their thickness profiles. Therefore, metrology tools with high accuracy and high measurement throughput are in great demand [1]. Current thickness profiling methods for 2D materials are limited in measurement throughput and accuracy. Here, we propose a high sensitivity transmission matrix based quantitative phase profilometry (TM-QPP), which is a high-speed and high-precision thickness profiling method [2]. In TM-QPP, picometer-level optical pathlength sensitivity is enabled in both temporal and spatial domains by extending the photon shot-noise limit of the high-sensitivity common-path interferometric microscopy configuration, while accurate thickness determination with ~ 10 pm precision is realized by developing a transmission-matrix model (Fig. 1(a)) that accounts for multiple refractions and reflections of light at sample interfaces. Using TM-QPP, the exact geometric thickness profiles of monolayer and few-layered 2D materials (e.g., MoS₂ in Fig. (b), (c) and WSe₂ in Fig. (d)) are mapped over a wide field of view within seconds in a contact-free manner. Meanwhile, TM-QPP can also spatially distinguish the number of layers of few-layered 2D materials (Fig. (e)-(f)).

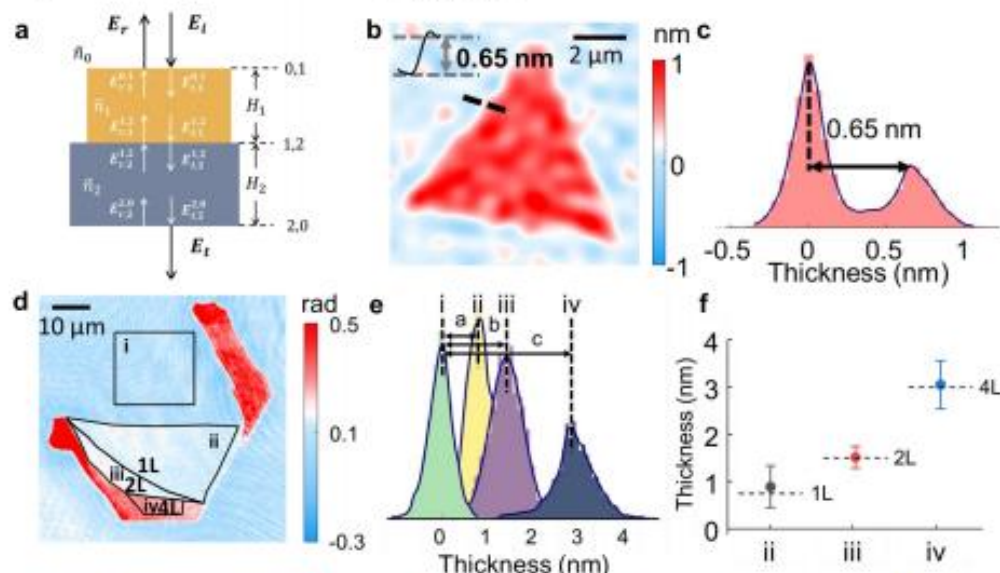


Fig. 1. (a) Transmission matrix model to accurately retrieve thickness of 2D materials. (b) Thickness map off monolayer MoS₂, and the thickness can be retrieved from the histogram shown in (c). (d) The phase map of the few-layered WSe₂ flake. (e) Thickness values calculated for each region with determined layer numbers based on the histogram in (e).

[1] D. Akinwande *et al.*, "Graphene and two-dimensional materials for silicon technology," *Nature* **573**, 507-518 (2019).

[2] Y. Nie *et al.*, "Transmission-Matrix Quantitative Phase Profilometry for Accurate and Fast Thickness Mapping of 2D Materials," *ACS Photonics* **10**, 1084-1092 (2023).

Photovoltaic-Based Visible Light Communications and its Alternate-Current Dynamics

Shuyan Chen and Lian-Kuan Chen

Department of Information Engineering, The Chinese University of Hong Kong, Hong Kong SAR, China
 Author e-mail address: {cs020, lkchen}@ie.cuhk.edu.hk

Abstract: This talk reports the characterization of photovoltaic (PV) cells' alternating current (AC) characteristics when working as passive photodetectors. The research content of this thesis is categorized into two parts: 1) the nonlinear optical-to-electrical (OE) characteristics of PV under low illuminance, and 2) the light-dependent dynamic frequency response of PV modules.

Photovoltaic visible light communication (PVLIC) is a promising technology that employs photovoltaic (PV) modules as a photodetector in visible light communication (VLC) receivers. The communication capability of PV modules using unbiased signal detection enables simultaneous energy harvesting and communication function. With the booming utilization of renewable power, photovoltaic (PV) modules are widely deployed for energy harvesting in many electronic devices. Extending PV's use to VLC applications attracts new research interest.

For PVLIC, the PV module's biasing conditions will influence its performance as a photodetector system. The solar panel can work in photoconductive mode (PC) and photovoltaic mode (PV). In PC mode, the reverse bias provides higher sensitivity, wider bandwidth, and improved linearity, as shown by the red line in Fig. 1(i). Conversely, no bias is applied in PV mode. Thus, it self-generates forward bias voltage. The solar panel often works in PV mode for energy harvesting; therefore, it is usually regarded as a direct-current (DC) component, and its DC characteristic is well-studied, while alternate-current (AC) characteristics are much less investigated.

In this workshop, we will report our work on developing new PVLIC models shown in Fig. 1(ii) [1],[2]. Our models accurately captures the frequency response dynamics (Fig. 1(iii)) and the nonlinear distortions (Fig. 1(iv)) due to PV mode characteristics. With the proposed models, communication performances are enhanced by reducing the bit error ratio and increasing data rate (Fig. 1(v)-(vi)).

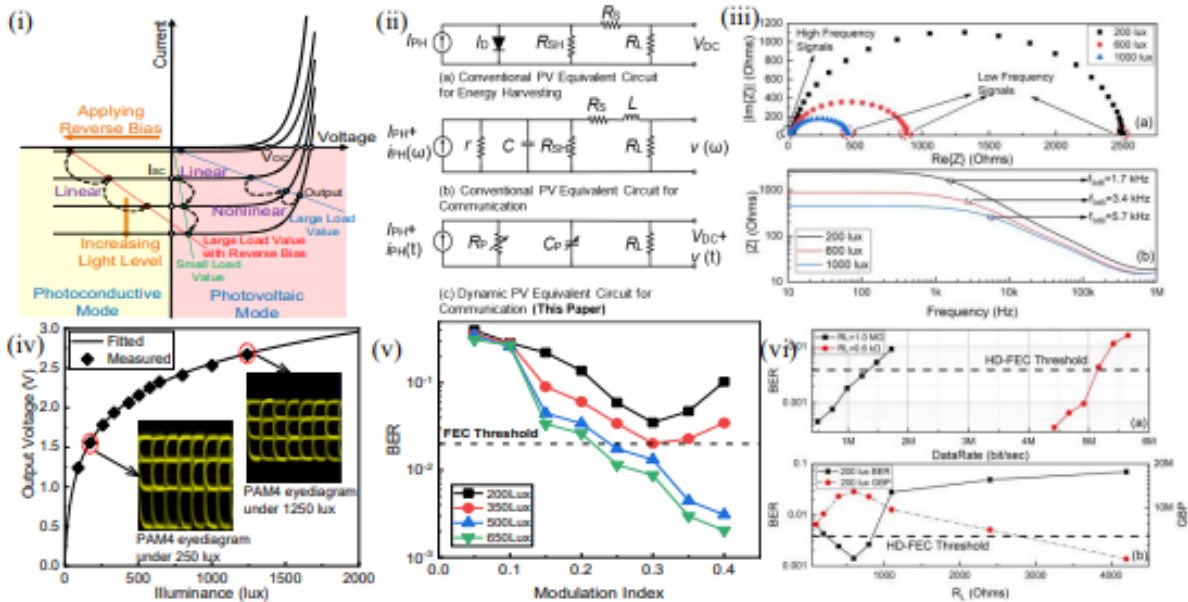


Fig. 1. (i) The photovoltaic O/E detection principle. (ii) A review chart on the development of photovoltaic AC model. (iii) Impedance dynamics of a PV module under different illuminance. (iv) DC response curve and signal distortion of a PV module. (v) BER reduction via nonlinear mitigation. (vi) Data rate enhancement via frequency response optimization.

References

- [1] S. Chen, L. Liu and L. -K. Chen, "On the Nonlinear Distortion Characterization in Photovoltaic Modules for Visible Light Communication," in *Photonics Technology Letters*, vol. 33, no. 24, pp. 1467-1470, 2021.
- [2] S. Chen, H. Yu, N. Zhao and L. -K. Chen, "A Dynamic Model for Frequency Response Optimization in Photovoltaic Visible Light Communication," in *Journal of Lightwave Technology*.

All-Optical Purification of Arbitrary Spectral Waveforms via Cross-Phase Modulation Based Talbot Amplifier

Zijian Li¹, Qijie Xie², Ziyue Zhang¹, Yuanfei Zhang¹, Honghui Zhang¹, and Chester Shu¹

¹Center for Advanced Research in Photonics, Department of Electronic Engineering, The Chinese University of Hong Kong, Shatin, N.T., Hong Kong

²Department of Mathematics and Theories, Peng Cheng Laboratory, No.2, Xingke 1st Street, Nanshan, Shenzhen, China
Author e-mail address: zijianli@link.cuhk.edu.hk

Abstract: Using cross-phase modulation-based Talbot amplifier, we achieve purification and in-band noise mitigation of broadband arbitrary spectral waveforms. The optical signal-to-noise ratio is improved by 9 dB, enabling recovery of spectral waveforms hidden under noise.

Noise mitigation is of great importance in different subject areas ranging from telecommunications, imaging, radio-astronomy, bio-sensing, to microwave photonics and others. Improving the signal quality and enhancing the optical signal-to-noise ratio (OSNR) are crucial for different optical systems [1]. In general, micro-ring resonators [2] and optical band-pass filters can purify signal for OSNR improvement. However, prior knowledge of the center frequency and bandwidth of the signal is required. To boost the signals, active optical amplifiers like erbium-doped fiber amplifiers (EDFA) are normally applied. Nevertheless, the OSNR might be degraded dramatically due to inherent amplified-spontaneous-emission noise. Recently, a passive amplification concept based on spectral Talbot array illuminator has been proposed and demonstrated for noise-less amplification of optical frequency combs [3] and spectral waveforms with frequency tones spaced by 10 MHz [4]. By using linear group velocity dispersion and electro-optic phase modulation, the signal under test (SUT) can be purified with improved OSNR. However, the operating rate is restricted by the electrical bandwidth of the phase modulator and the sampling rate of the electrical waveform generator. Electro-optic modulation can barely take effect in achieving significant OSNR improvement for a SUT with frequency tones spaced wider than a few GHz due to the requirement on implementing ultrafast step-like phase profiles. In this work, we develop an all-optical method to purify arbitrary broadband spectral waveforms through the synergy of cross-phase modulation (XPM) and spectral Talbot effect. Figure 1 illustrates the principle. A noise-overwhelmed optical spectral waveform served as a SUT (with an in-phase temporal counterpart as an example) is indicated by red lines. The SUT propagates through a dispersive medium providing group velocity dispersion [4]. Consequently, a temporally periodic phase pattern is imposed on the SUT. To compensate for the parasitic temporal phases, nonlinear XPM is performed to impart an opposite temporal phase to the SUT. The target intensity profiles of the pump can be generated by line-by-line spectral shaping via an optical WaveShaper [5-7]. The phase compensation through the XPM process leads to a coherent consecutive sum of the SUT, while the stochastic noise stays unaltered. Hence, the energy of the SUT is redistributed to generate an OSNR-boosted spectral sampling peaks with preserved spectral envelope. The approach can be applied to improve the signal quality in different optical communication and sensing systems.

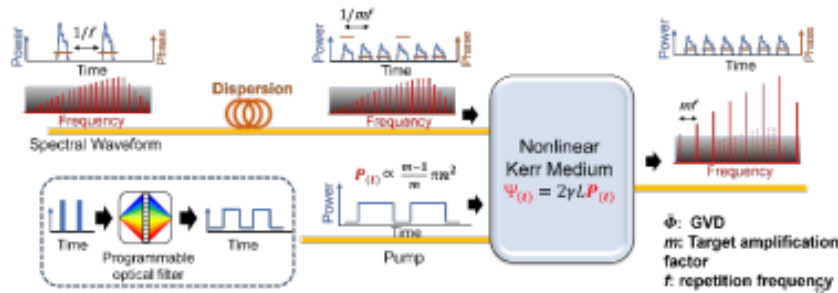


Fig. 1. Operating principle for purification of optical spectral waveform via XPM-based Talbot amplifier. λ_1 : center wavelength of the noisy signal. λ_2 : center wavelength of the pump.

References

- [1] Radan Slavik, et al, Nature Photon **4**, 690–695 (2010).
- [2] Chawaphon Prayoonpong, et al, JLT **39**, 7383-7392 (2021).
- [3] Luis Romero Cortés, et al, Phys. Rev. Applied **9**, 064017 (2018).
- [4] Benjamin Crockett, et al., Nat Commun **12**, 2402 (2021).
- [5] Ferdous Fahmida, et al., Nature Photon **5**(12), 770-776 (2011).
- [6] Manuel P. Fernández, et al., Opt. Lett. **45**, 3557-3560 (2020)
- [7] Manuel P. Fernández, et al., in CLEO, 2022, paper SM2O.5.

In-plane 1.5 μm DFB lasers on SOI for integrated photonics

Ying Xue¹, Jie Li¹, Yi Wang², Ke Xu¹, Zengshan Xing³, Kam Sing Wong³, Hon Ki Tsang², Kei May Lau^{1,2*}

¹Department of Electronic and Computer Engineering, Hong Kong University of Science and Technology, Clear Water Bay, Kowloon, Hong Kong, China

²Department of Electronic Engineering, The Chinese University of Hong Kong, Hong Kong, China

³Department of Physics and William Mong Institute of Nano Science and Technology, Hong Kong University of Science and Technology, Clear Water Bay, Kowloon, Hong Kong, China
kmlau@ee.cuhk.edu.hk, eekmlau@ust.hk

Abstract: We report 1.5 μm distributed feedback lasers laterally grown on industry-standard (001)-oriented silicon-on-insulator wafers for integrated photonics. The lasers feature a co-planar configuration with the Si device layer and a low lasing threshold of 17 $\mu\text{J}/\text{cm}^2$. © 2023 The Author(s)

1. Introduction

Silicon photonics stands as a pivotal technology revolutionizing data communication and enabling various emerging applications [1]. Despite the remarkable success of Si passive components, the monolithic integration of III-V lasers onto Si substrates has posed a significant challenge. Traditional blanket epitaxy produces lasers on Si via the growth of thick III-V buffer layers, essential for defect reduction, yet this technique impedes the efficient coupling between III-V lasers and Si waveguides. To address this intricate conundrum, our research has yielded an innovative solution in the form of “lateral aspect ratio trapping” (LART), a distinctive selective epitaxy method eliminating III-V buffer layers. Using LART, we have achieved a co-planar configuration of III-V devices alongside Si, leading to efficient light coupling between III-V and Si counterparts [2]. Here, leveraging a unique grating design and significantly enlarged III-V material volume, we present DFB lasers laterally grown on (001) silicon-on-insulator (SOI) wafers.

2. Results and Discussion

After preparing SOI template [3], we performed lateral selective epitaxy in an AIXTRON closed-couple-showerhead metal-organic chemical vapor deposition (MOCVD) system with optimized growth parameters for large III-V volume and uniform morphology. The as-grown quantum wells (QWs) exhibit high crystalline quality without observable threading dislocations (TDs), grain boundaries, antiphase boundaries, or twins (Fig. 1(a)). We fabricated gratings with a pitch of 310 nm, a duty cycle of 50% and a width of 400 nm to provide sufficient reflections at 1.5 μm , reduce non-radiative recombination and simplify the fabrication process simultaneously (Fig. 1(a)). During the measurement, with the increase of pumping level, a mode at 1.5 μm gradually dominated the emission spectrum and finally lased as depicted in Fig. 1(b). The lasing mode demonstrates a side mode suppression ratio (SMSR) of 35 dB. The threshold was extracted to be around 17 $\mu\text{J}/\text{cm}^2$ from the light-light ($L-L$) curves in Fig. 1(c).

3. Conclusion

In conclusion, we demonstrated 1.5 μm DFB lasers laterally grown on (001) Si-photonics SOI, featuring co-planar structure with Si, a low lasing threshold of 17 $\mu\text{J}/\text{cm}^2$, single-mode lasing at 1.5 μm with an SMSR of 35 dB and a high spontaneous emission factor of 0.7.

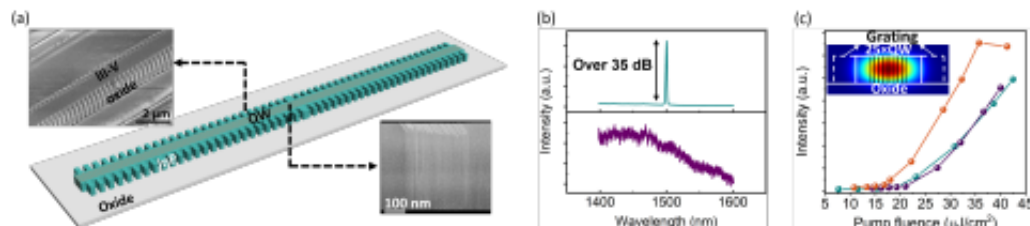


Fig. 1 (a) 3D architecture of the DFB laser on SOI including TEM image of the as-grown QWs at the center of the DFB laser cavity and the tilted view SEM image showing the gratings with uniform pitch and smooth sidewall. (b) Spectrum of the DFB laser on SOI measured below and above threshold. (c) $L-L$ curves of the DFB lasers on SOI, inset: cross-sectional view of corresponding lasing mode in the DFB lasers.

4. References

- [1] M. Near, et al., “Perspective on the future of silicon photonics and electronics.” *Applied Physics Letters*, 118(22), 220501, 2021.
- [2] Y. Xue, et al., “High-speed and low dark current silicon-waveguide-coupled III-V photodetectors selectively grown on SOI”, *Optica*, 9(11), 1219-1226, 2022.
- [3] Y. Xue, et al., “High-performance III-V photodetectors on a monolithic InP/SOI platform”, *Optica*, Vol. 8, no. 9, pp. 1204-1209, 2021.

A Digital Signal Processing Perspective on Enhancing Capacity and Security of Bandwidth-Limited LED/Laser Communication Systems

Geyang Wang, Lian-Kuan Chen

Department of Information Engineering, The Chinese University of Hong Kong, Hong Kong SAR, China

Abstract: In order to improve the capacity and security of bandwidth-limited optical communication systems, we propose various precoding schemes. The experiments show our scheme can obtain 8.8% capacity improvement, a considerable spectral saving of $\sim 12\%$, and $\sim 10^{88}$ key space (KS). © 2023 The Author(s). e-mail address: wg022@ie.cuhk.edu.hk

Content-rich applications drive the substantial growth in IMDD Communication system, resulting in ever-growing capacity demand. However, capacity enhancement is significantly hampered by power fading issues arising from chromatic dispersion and bandwidth limitations in existing IMDD systems. We first propose a general framework based on perfect polyphase sequences (PPS) to consolidate existing precoding strategies, with a lot of precodings being its special cases. We further propose a PPS-circulant matrix-based Faster-than-Nyquist (PPS-CrM FTN) system that employs PPS-CrM with different compression factors for the FTN function, which can achieve a great spectral saving of $\sim 12\%$ and better capacity improvement [1]. Meanwhile, with the broadcasting nature in the downstream link of the OFDM-PON systems, the information integrity is more susceptible to both eavesdroppers and illegal optical network units. We proposed a new physical layer encryption scheme for simultaneous improvement of capacity and security, which can further supply huge key space [2].

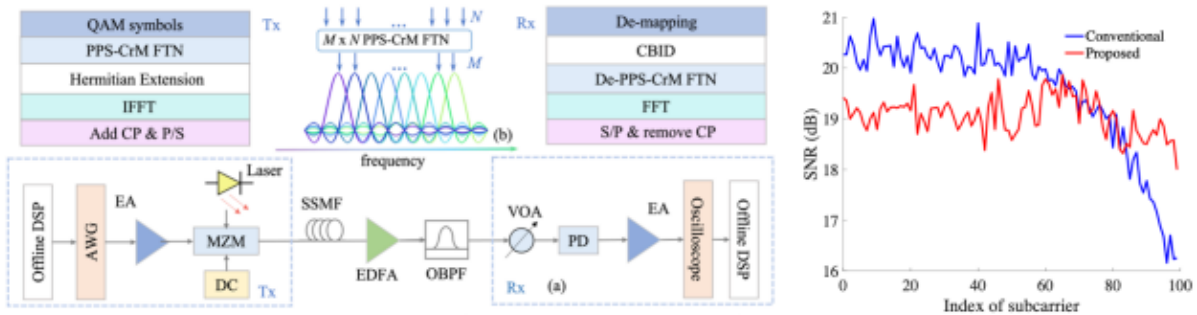


Fig. 1. (a) Principle and experimental setup of proposed PPS-CrM FTN, (b) proposed $M \times N$ PPS-CrM FTN signal, and (c) the SNR-profile with proposed schemes. (AWG: arbitrary waveform generator. EA: electrical amplifier. MZM: Mach-Zehnder modulator. SSMF: standard single-mode fiber. EDFA: erbium-doped fiber amplifier. OBPF: optical bandpass filter. VOA: variable optical attenuator. PD: photodiode.)

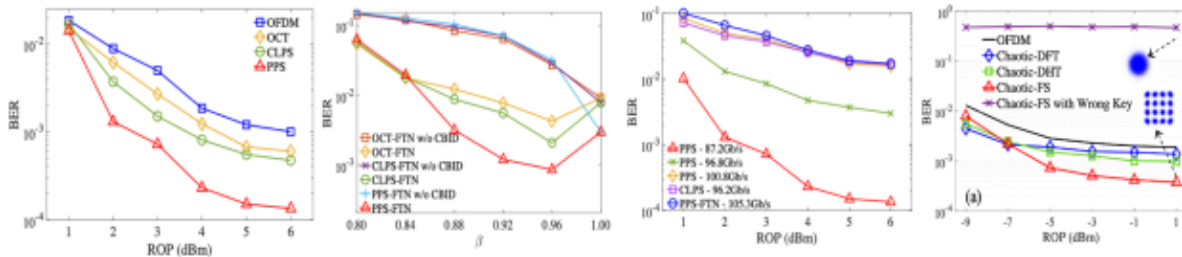


Fig. 2. BER versus the (a) ROP at 87.2Gb/s, (b) the compress factor β at 87.2Gb/s, (c) the ROP at different data rates, and (d) ROP using different security schemes and the constellation diagrams.

[1] G. Wang et al., ECOC, (2023)

[2] G. Wang et al., CLEO, SF2M. 5 (2023)

Random Access Particle Tracking

Yintao Wang, Bingxu Chen, and Shih-Chi Chen*

Department of Mechanical and Automation Engineering, The Chinese University of Hong Kong, Hong Kong, China

*Author e-mail address: scchen@mae.cuhk.edu.hk

Abstract: In this letter, we propose a multi-target particle tracking system based on digital micromirror device (DMD). This system outperforms most current systems in maximum tracking speed and concurrent target quantity while maintaining the system accuracy and precision in 10-nanometer scale.

1. Introduction

The emergence of single particle tracking (SPT) spectroscopy brings about the ability to detect individual particle dynamics in both biological and physical systems. However, current SPT systems can only track single particle moving slower than $10 \mu\text{m/s}$ [1]. To address this issue, we developed a 3D scanning system based on digital micromirror device (DMD) and Lee holography. Thanks to the ultra-high speed performance and ultra-large scan range, multiple target particle can be monitored at the same time and the max tracking speed can reach $\sim 200 \mu\text{m/s}$.

2. Results

2.1 Software and hardware setups

According to Lee holography, the on-off states of each DMD pixel can be independently calculated according to the location of target foci. The solution to this highly parallel equation for generating DMD holograms can be accelerated by a GPU. The tested hologram rendering speed reaches over 8000 fps (Fig. 1b).

To test system efficacy, we have built up several DMD-based FD-SPT systems. The most compact setup only uses 5 optical components to realize 3D random access scanning. A typical system is shown in Fig 1a. The feedback fluorescent signals are acquired via a PMT and FPGA module. Additional piezoelectric stage and linear stage are used to test the accuracy/precision and expand the tracking range to millimeter range, respectively.

2.2 System performance

The system performance is tested in multiple aspects such as accuracy, maximum tracking speed, tracking range, step resolution, multi-target performance, etc. The tracking range ($50 \times 50 \times 50 \mu\text{m}^3$) and accuracy ($< 100 \text{ nm}$) is shown in Fig. 1d. The multi-target capability and tracking speed ($\sim 200 \mu\text{m/s}$) is shown in Fig. 1c. By this system, we are able to monitor the Brownian motion of a 100 nm nano diamond in DI water (Fig. 1e).

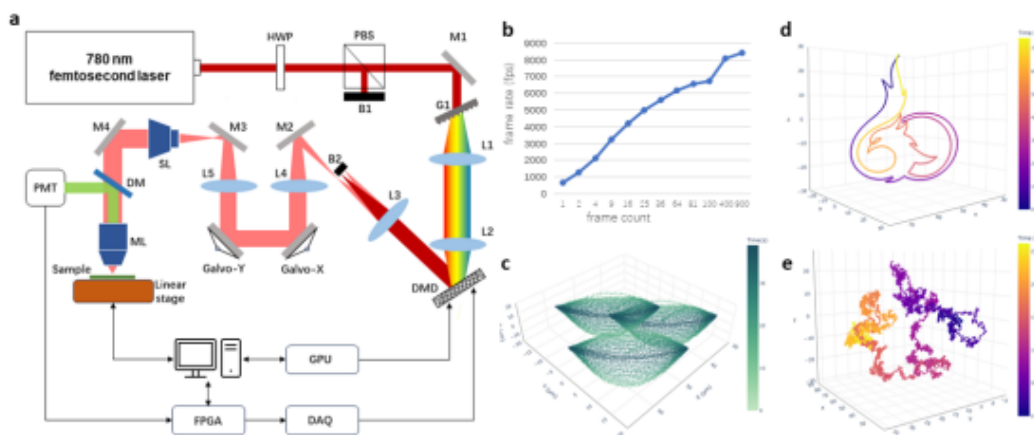


Fig. 1. The design and performance of the DMD-based random access tracking system.

3. References

- [1] B. Van Heerden, et al., "Real-time feedback-driven single-particle tracking: a survey and perspective," *Small* **18.29**, 2107024 (2022).

Ultrahigh-resolution Miniaturized Visible-light Optical Coherence Tomography Endoscopy

Chao Xu, Tinghua Zhang, Peng Liu, Wu Yuan*

Department of Biomedical Engineering, The Chinese University of Hong Kong, Hong Kong SAR, China
 Author e-mail address: wyuan@cuhk.edu.hk

Endoscopic optical coherence tomography (OCT) offers near-histologic quality visualization of tissue microanatomy *in vivo*, overcoming the limitations of traditional biopsy methods by enabling volumetric sampling without necessitating tissue removal. Clinical applications, such as intravascular imaging, need imaging probes of high resolution and small form size. As an emerging technique, visible light OCT (vis-OCT) endoscopy holds significant promise for achieving ultrahigh resolution ($\sim 1 \mu\text{m}$) and enhanced image contrast and providing spectroscopic sensitivity to hemoglobin oxygenation for evaluating functional physiopathology *in vivo*.

However, current vis-OCT endoscopes based on achromatic lenses and distal motors present challenges in terms of bulkiness and safety concerns in clinical settings, highlighting the needs for ultracompact and current-free alternatives. Conventional fabrication methods for ultrathin vis-OCT endoscopes also face performance limitations. For instance, traditional gradient-index (GRIN) fiber-based probes introduce chromatic aberration in visible light, which compromises axial resolution, while the fiber-melting method lacks the flexibility to customize the ball-lens on the probe tip. Two-photon polymerization method prints a microlens with sufficient design of freedom, but its optical surface roughness is still suboptimal for OCT imaging at visible light.

In this study, we introduce the first submillimeter monolithic vis-OCT endoscope, achieved by directly fabricating a microlens on the fiber tip. Our proposed method capitalizes on the self-assembly properties of curable optical liquid on a wettability-modified substrate to create a liquid lens. This approach enables convenient customization of the liquid lens in shape and size by tailoring the liquid volume and substrate wettability. The resulting liquid-shaped lens boasts an ultra-smooth surface with subnanometer roughness, which helps reduce unwanted scattering in the visible spectrum and enhances image quality. The ultrathin vis-OCT endoscope, with an outer diameter of 0.6 mm, delivers an aberration-corrected imaging performance and facilitates ultrahigh-resolution ($1.2 \mu\text{m} \times 4.5 \mu\text{m}$ in axial and transverse directions) structural and functional imaging in luminal organs *in vivo*, while minimizing invasiveness. This innovative approach represents a significant advancement in endoscopic imaging techniques and holds considerable potential for impacting clinical applications. By leveraging the unique properties of curable optical liquid and wettability-modified substrates, our method offers a promising solution for the development of compact, high-performance endoscopic imaging devices.

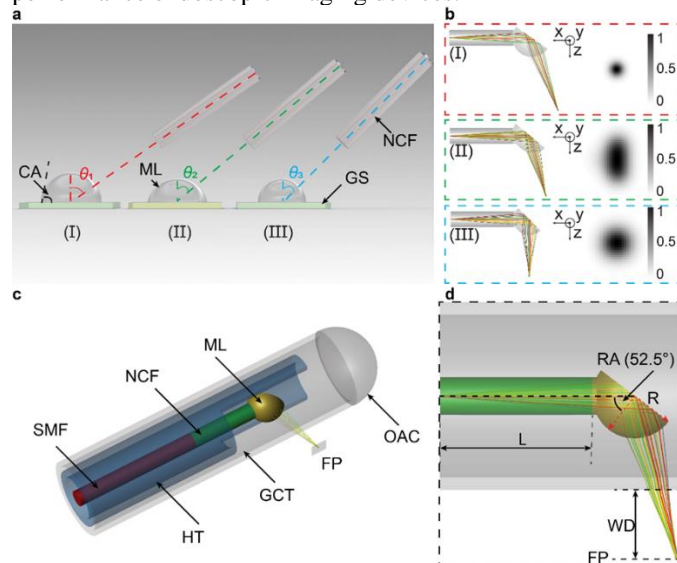


Fig. 1 Design of liquid-shaped micro-endoscope. a. Concept of liquid-shaped imaging probe. Optical liquids on the glass substrates with various wetting properties (indicated by different colors, that is, green for (I) and (III), and yellow for (II)) form the micro-lenses with different contact angles, thus different shapes. b. Focused spot positions and sizes under different configurations. c. Schematic of liquid-shaped micro-endoscope. d. Close view of the micro-endoscope. CA: contact angle, ML: micro-lens, GS: glass substrate, NCF: non-core fiber, SMF: single-mode fiber, HT: hypodermic tube, GCT: glass capillary tube, OAC: optical adhesive cap, RA: reflection angle, FP: focal plane. WD: working distance.

1. Duan, L. et al. Colposcopic imaging using visible-light optical coherence tomography. *J Biomed Opt* 22, 56003, doi:10.1117/1.JBO.22.5.056003 (2017).
2. Winkelmann, J. A. et al. In vivo broadband visible light optical coherence tomography probe enables inverse spectroscopic analysis. *Opt Lett* 43, 619-622, doi:10.1364/OL.43.000619 (2018).

A power efficient and high precision micro-ring weight bank sparsity resolving the thermal challenges

Tengji Xu,¹ Weipeng Zhang,² Qiarong Xiao,¹ Benshan Wang,¹ Mingcheng Luo,¹ Bhavin J Shastri,³ Paul Pruncal,² and Chaoran Huang^{1,*}

¹ Department of Electronic Engineering, The Chinese University of Hong Kong, Shatin, Hong Kong SAR, China

² Department of Electrical and Computer Engineering, Princeton University, Princeton, 08544, NJ, USA

³ Department of Physics, Engineering Physics & Astronomy, Queen's University, Kingston, K7L 3N6, ON, Canada

* crhuang@ee.cuhk.edu.hk

Abstract: A hardware-algorithm codesign-based in-silico training method is proposed can significantly improve photonic neural networks inference accuracy and reduce operation power. © 2023 The Author(s)

Micro-ring resonator (MRR) weight bank based Photonic neural network is a common approach to implement photonic synapses [1]. MRR weight bank offers distinct advantages including power-efficient tuning, straightforward weight assignment, and high computing density. However, MRRs are highly susceptible to thermal fluctuations. Current control methods incur additional hardware costs and increase system complexity [2-4]. We propose a hardware-algorithm codesign-based approach that does not introduce additional hardware complexity to address these challenges. This is achieved by enforcing most weight values to a thermally-insensitive operational region of MRRs when training the PNNs. This concept shares similarities with NN pruning in digital hardware [5]. Importantly, this thermally-insensitive region coincides with the region requiring minimal control power for weight assignment. As a result, our approach also leads to a substantial power consumption reduction. We experimentally demonstrated our proposed method can increase a two layer CNN MNIST classification accuracy from 77.48% to 96.42% with 10 times power reduction, simulation verified it can increase LeNet-5 MNIST classification accuracy from 12.99% to 97.97% with 22 times power reduction and ResNet-18 CIFAR-10 classification accuracy from 8.31% to 80.83% with 112 times power reduction.

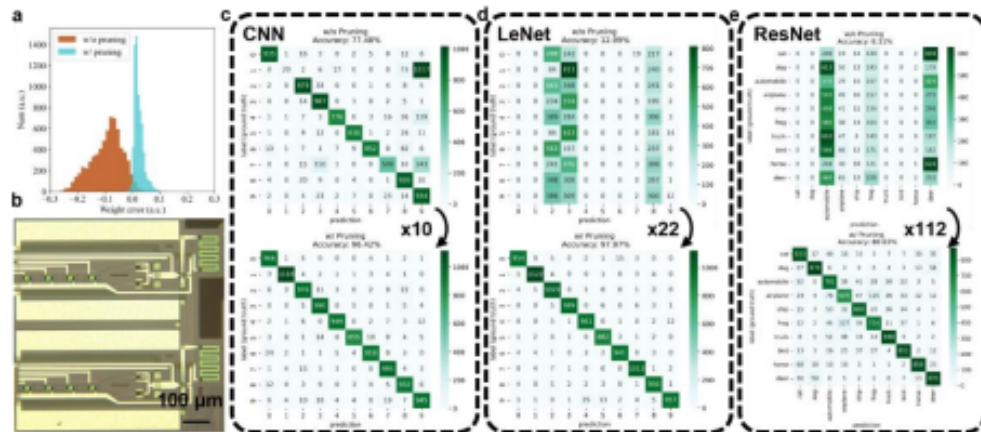


Fig. 1. Experiment results and picture. (a) Experiment weight error histogram. (b) Experiment MRR weight bank. (c) Two-layer CNN confusion matrix with 10 times power reduction. (d) LeNet confusion matrix with 22 times power reduction. (e) ResNet confusion matrix with 112 times power reduction.

References

- [1] Zhang, W., Tait, A., Huang, C. et al. Broadband physical layer cognitive radio with an integrated photonic processor for blind source separation. *Nat Commun* **14**, 1107 (2023).
- [2] Huang, Chaoran, et al. "Demonstration of scalable microring weight bank control for large-scale photonic integrated circuits." *APL Photonics* **5.4** (2020).
- [3] Weipeng Zhang, Chaoran Huang, Hsuan-Tung Peng, Simon Bilodeau, Aashu Jha, Eric Blow, Thomas Ferreira de Lima, Bhavin J. Shastri, and Paul Pruncal, "Silicon microring synapses enable photonic deep learning beyond 9-bit precision," *Optica* **9**, 579-584 (2022)
- [4] Qingming Zhu, Ciyuan Qiu, Yu He, Yong Zhang, and Yikai Su, "Self-homodyne wavelength locking of a silicon microring resonator," *Opt. Express* **27**, 36625-36636 (2019).
- [5] Frankle, Jonathan, and Michael Carbin. "The lottery ticket hypothesis: Finding sparse, trainable neural networks." *arXiv preprint arXiv:1803.03635* (2018).

On chip photothermal spectroscopy for gas detection

Yue Yan,^{1,*} Wei Ren¹

¹Department of Mechanical and Automation Engineering, The Chinese University of Hong Kong, New Territories, Hong Kong SAR, China
Author e-mail address: yanyue@link.cuhk.edu.hk

Abstract: We proposed sensitive on chip photothermal spectroscopy (PTS) for gas detection on a ring resonator. It provides a new opportunity for future on-chip gas sensor development with high sensitivity and selectivity. © 2023 The Author(s)

In a typical photothermal spectroscopy (PTS) system with a pump-probe configuration ^[1], gas absorption of the modulated pump light dissipates periodic heat to surroundings and subsequently changes the refractive index (RI) of the gas medium. The RI variation modulates the phase of a probe laser that propagates through the same path as the pump laser in the gas medium. The photothermal sensitivity depends strongly on the pump laser intensity. Hence, the tightly confined optical field on a sub-micrometer waveguide can significantly enhance the pump laser intensity for a stronger photothermal effect.

Fig.1 depicts the schematic of a PTS system for gas detection on an integrated ring resonator. The pump beam and probe beam are coupled inside the ring resonator using a wavelength division multiplexer (WDM). At the output, another WDM splits the pump and probe to the photodetectors. The pump resonance can be tuned to be exactly located at the peak of the gas absorption spectrum. At the center resonance, the pump intensity can be largely enhanced to produce significant photothermal effect induced by the gas absorption of the evanescent field. This photothermal effect will bring refractive index change of the ring resonator, thus shifting the resonance position of a probe beam. As shown in Fig.1, in the probe resonance, the probe wavelength can be locked at the slope of the resonance. Small resonance position shift will produce large amplitude change.

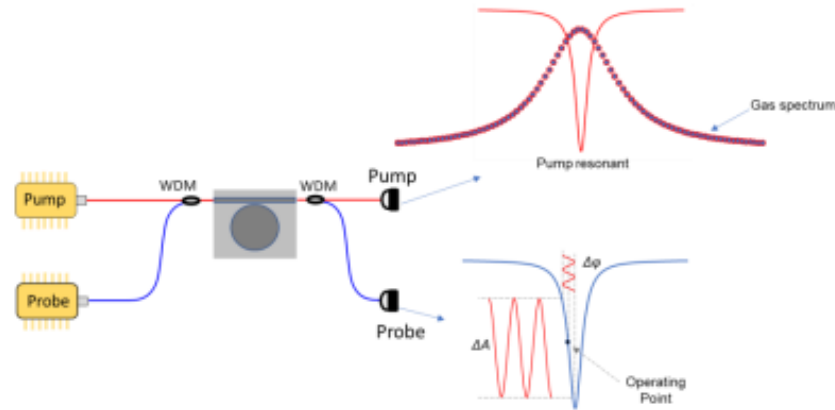


Fig. 1 Schematic of the PTS system for gas detection on an integrated ring resonator.

The proposed on-chip PTS can be used for gas detection with highly sensitive and selectivity. It should be note that the ring resonator may have intrinsic photothermal effect that could overthrow the photothermal signal of the analyte gas. So, selecting a proper material with negligible thermo-optic effect is very important.

3. References

[1] Wang, Q., Wang, Z., Zhang, H., Jiang, S., Wang, Y., Jin, W., and Ren, W. (2022). Dual-comb photothermal spectroscopy. *Nature Communications*, 13(1), 2181.

A steerable OCT endoscope using pneumatic motor

Tinghua Zhang¹, Chao Xu¹, Peng Liu¹, Sishen Yuan², Hongliang Ren², Wu Yuan^{1*}

¹ The Chinese University of Hong Kong, Department of Biomedical Engineering

² The Chinese University of Hong Kong, Department of Electronic Engineering

* Corresponding author: Wu Yuan, mail: wyuan@cuhk.edu.hk.

Abstract:

Optical coherence tomography (OCT) endoscopy is increasingly utilized in clinic to provide high-resolution diagnostic images (or optical biopsy) of the diseased tissues in luminal organs [1,2]. The premier clinical applications of OCT endoscope include the evaluation of cardiovascular diseases and the intravascular stent strut assessment. Currently, OCT endoscopes mainly employ a torque coil to perform the proximal scanning for circumferential imaging. However, the proximal-scanning OCT endoscope suffers from so-called non-uniform rotational distortion (NURD) in tortuous lumens. Although the alternative distal-scanning method utilizing a micromotor in the OCT endoscope can effectively mitigate the NURD issue, there are still safety concerns of the thermal and electrical issues in clinic. Moreover, to precisely navigate the OCT endoscope to the suspected regions in a complex organ, the controllability and steerability of endoscope are highly desirable[3].

In this work, we develop a steerable OCT endoscope to perform distal scanning using an electrical-free pneumatic motor for NURD-free high-resolution imaging in the convoluted lumens, such as pulmonary airways (Fig. 1). The performance of the pneumatic motor and the steerability of endoscope has been optimized and characterized. The experimental results demonstrate that the proposed endoscope can perform stable circumferential imaging at a speed from about 60 to 100 Hz and provide a maximum bending angle of up to 150 degrees. Using animal models and airway phantoms, the proposed endoscope was further validated to navigate and perform targeted NURD-free high-resolution imaging in the complex luminal system.

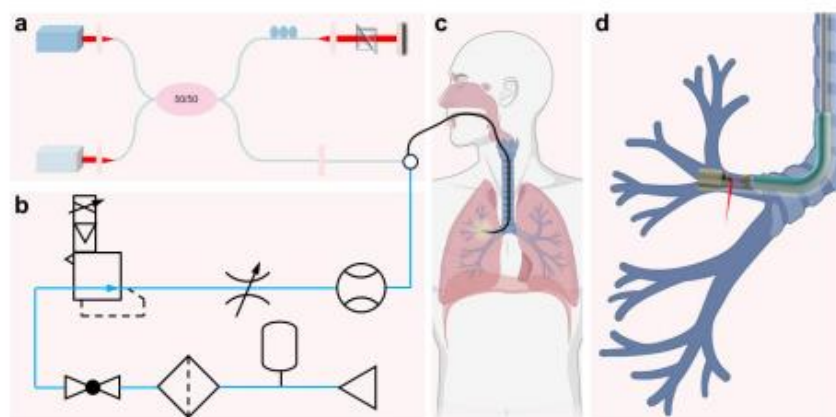


Fig. 1. Schematic of the proposed OCT endoscope.

References

- [1] Yuan, Wu, et al. "Super-achromatic monolithic microprobe for ultrahigh-resolution endoscopic optical coherence tomography at 800 nm." *Nature communications* 8.1 (2017): 1531.
- [2] Yuan, Wu, et al. "Theranostic OCT microneedle for fast ultrahigh-resolution deep-brain imaging and efficient laser ablation in vivo." *Science advances* 6.15 (2020): eaaz9664.
- [3] A. Alian, E. Zari, Z. Wang, E. Franco, J. P. Avery, M. Runciman, B. Lo, F. R. y Baena, and G. Mylonas, "Current engineering developments for robotic systems in flexible endoscopy," *Techniques and Innovations in Gastrointestinal Endoscopy*, 2022.

Scan-less phase imaging based on a single-cavity dual-comb laser with spatiotemporal encoding

Zhiwei Zhu¹, Wanping Lu¹, and Shih-Chi Chen¹

¹Department of Mechanical and Automation Engineering, The Chinese University of Hong Kong, Shatin, N.T., Hong Kong SAR, China
Author e-mail address: zhiweizhu@cuhk.edu.hk

Abstract: We present a novel scan-less phase imaging microscope system based on a compact single-cavity dual-comb laser with the spatiotemporal encoding method. Our system achieves a frame rate of 330 Hz, with 676×32 pixels and the phase resolution of 0.082 rad for scan-less phase imaging in the field of view (FOV) of 230 μm×200 μm. © 2023 The Author(s)

Measuring optical phase to enable the phase imaging for samples is a very meaningful technique to give the information on refractive index, optical thickness, geometrical shape and to visualize transparent non-fluorescent objects or reflective objects with nanometer unevenness. The dual-comb interferometer is an effective approach to achieve direct phase measurement and naturally provides over hundreds, or even more, frequency channels for precise measurements. To reduce or even eliminate the mechanical scanning for ultrafast scan-less imaging, the scan-less confocal phase imaging based on dual-comb microscopy with 2D spectral encoding has been reported [1], which applies a fully stabilized dual-comb source but is complex and expensive. Here, we present a novel scan-less dual-comb microscopy technique based on a compact single-cavity dual-comb laser with spatiotemporal encoding.

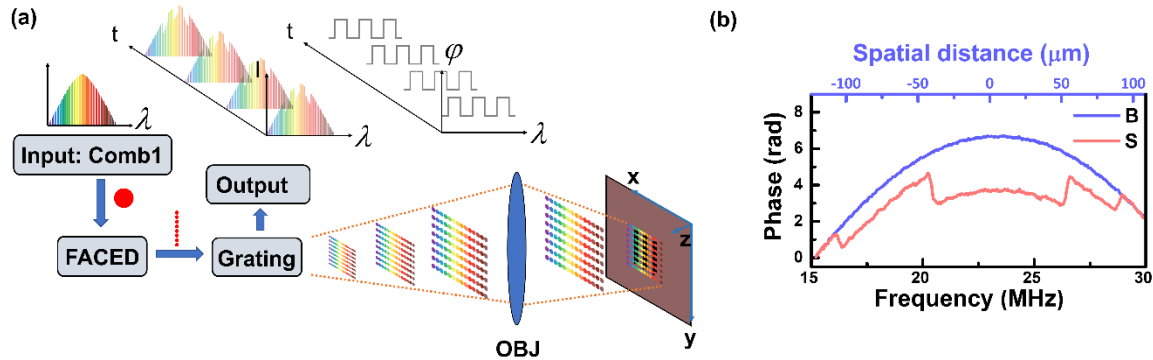


Fig. 1. (a) Spatiotemporal encoding on a dual-comb laser for scan-less phase imaging. (b) Phase imaging for the sample with a two-step structure.

By simultaneously utilizing time-to-space and wavelength-to-space conversation in two orthogonal directions, a new 2D spectral encoding has been realized. Figure 1(a) illustrates the principle of our spatiotemporal encoding method. The optical frequency comb is first time-to-space encoded and space-encoded by a free-space angular-chirp-enhanced delay (FACED) device [2], to generate an optical line with a series of discrete points in the vertical direction (Y-axis). Then, a diffraction grating is used in the horizontal direction (X-axis) to unfold the spectrum of each spot and generate a 2D line-array. The 2D line-array provides self-scanning along Y-axis without extra mechanical scanning and enables scan-less imaging. By slicing and decoding the IGMs in different time channels, the amplitude and phase spectra of each line can be obtained to reconstruct 2D and 3D images of samples. Figure 1(b) show the phase spectra a single line spanning across the two-step sample and the corresponding background after normalization. The standard deviations of phase values are 0.082 rad for 3 ms, 0.041 rad for 15 ms, 0.024 rad for 90 ms, which correspond to the depth resolution of 6.86 nm, 3.43 nm, 2.01 nm, respectively.

References:

10. E. Hase, T. Minamikawa, T. Mizuno, S. Miyamoto, R. Ichikawa, Y.-D. Hsieh, K. Shibuya, K. Sato, Y. Nakajima, A. Asahara, K. Minoshima, Y. Mizutani, T. Iwata, H. Yamamoto, and T. Yasui, "Scan-less confocal phase imaging based on dual-comb microscopy," *Optica* 5, 634 (2018).
- J. Wu, Y. Xu, J. Xu, X. Wei, A. C. Chan, A. H. Tang, A. K. Lau, B. M. Chung, H. C. Shum, E. Y. Lam, K. K. Wong, and K. K. Tsia, "Ultrafast laser-scanning time-stretch imaging at visible wavelengths," *Light: Science & Applications* 6, e16196 (2017).

In vivo ultrahigh-resolution imaging in airways using 800-nm OCT endoscopy

Peng Liu¹, Chao Xu¹, Tinghua Zhang¹, Sishen Yuan², Wu Yuan^{1*}

¹ Department of Biomedical Engineering, The Chinese University of Hong Kong, Hong Kong SAR, China.

² Department of Electronic Engineering, The Chinese University of Hong Kong, Hong Kong SAR, China.

*wyuan@cuhk.edu.hk

Abstract:

Asthma is one of the most common respiratory diseases and 5-10% of asthmatics suffer from severe asthma. Recently, bronchial thermoplasty (BT) and targeted lung denervation (TLD) have been developed for managing severe asthmatics in addition to biologic. BT utilizes radiofrequency energy to reduce airway smooth muscle (ASM) in airways, while TLD works on the deactivation of pulmonary nerves to relieve airway constriction. However, variant efficacy of these methods was identified and may associate with different phenotypes of severe asthma. On the other hand, previous studies have shown that ASM can be an effective biomarker in characterizing asthmatic phenotypes and severities [1-3]. However, *in vivo* imaging and quantification of ASM in airways remains challenging.

Endoscopic optical coherence tomography (OCT) enables the high-resolution three-dimensional imaging in luminal organs. It has been demonstrated before that endoscopic OCT is able to visualize airway anatomy *in vivo*. However, the resolution and contrast of conventional endoscopic OCT at 1300 nm is still suboptimal to directly resolve ASM in airways *in vivo*. Therefore, we developed an endoscopic OCT system operating at 800 nm to provide an ultrahigh resolution of about 1.7 μm (in tissue) with an enhanced imaging contrast. We performed imaging study of airways in animals and found that the airway microstructures, including ASM, can be clearly identified in OCT images (see Figure 1). In addition, a new method for automated 3D segmentation and quantification of OCT images was developed. The thickness and area of each tissue component in airways can be accurately measured [2]. This new imaging technique has the potential to stratify severe asthma for effective phenotyping and treatment.

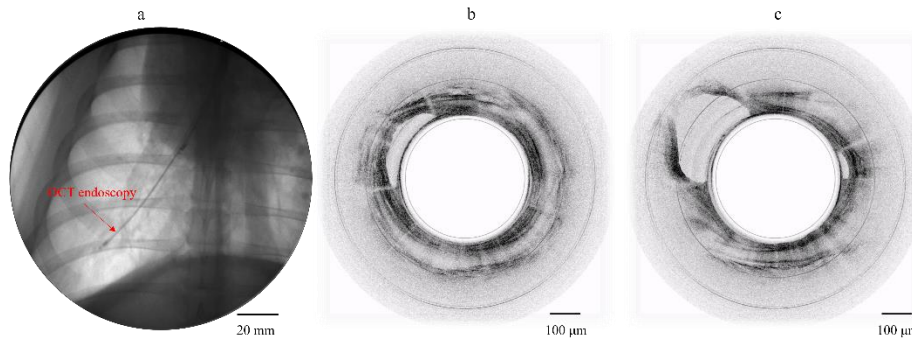


Fig. 1. OCT endoscopy in pig lung and representative OCT airway images.

References

- [1] Jeffrey Thiboutot, Wu Yuan, Hyeon-cheol Park, Dawei Li, Jeffrey Loube, Wayne Mitzner, Lonny Yarmus, Xingde Li, Robert H. Brown, Visualization and Validation of The Microstructures in The Airway Wall *in vivo* Using Diffractive Optical Coherence Tomography, *Academic Radiology*, 29 (11), 11623-1630 (2022).
- [2] Yuan, W., Thiboutot, J., Park, H., Li, A., Loube, J., Mitzner, W., Yarmus, L., Brown, R.H., and Li, X., Direct Visualization and Quantitative Imaging of Small Airway Anatomy Using Deep Learning Assisted Diffractive OCT, *IEEE Transactions on Biomedical Engineering*, 70(1), 238-246 (2022).
- [3] F. Ladouceur and J. D. Love, *Silica-based buried channel waveguides and devices* (Chapman & Hall, 1995), Chap. 8 Adams DC, Hariri LP, Miller AJ, Wang Y, Cho JL, Villiger M, Holz JA, Szabari MV, Hamilos DL, Scott Harris R, Griffith JW, Bouma BE, Luster AD, Medoff BD, Suter MJ., Birefringence microscopy platform for assessing airway smooth muscle structure and function *in vivo*, *Science Translational Medicine*, 8(359), 131 (2016).

Optical Metasurfaces for Medical Image Classification

Mingcheng Luo¹, Meirui Jiang², Wenfei Guo¹, Tengji Xu¹, Nansen Zhou³, Dongliang Wang¹, Renjie Zhou³, Qi Dou², Chester Shu¹, and Chaoran Huang^{1*}

¹Department of Electronic Engineering, The Chinese University of Hong Kong, Shatin, Hong Kong, China

²Department of Computer Science and Engineering, The Chinese University of Hong Kong, Shatin, Hong Kong, China

³Department of Biomedical Engineering, The Chinese University of Hong Kong, Shatin, Hong Kong, China

* Corresponding author. Email: crhuang@ee.cuhk.edu.hk

Abstract: We experimentally demonstrate a metasurface-based optical neural network for medical image classification. The performance is comparable to that of the state-of-art digital neural network while digital parameters can be reduced by 10^3 to 10^5 times.

Free-space-based optical neural networks can directly process input images in the optical domain with nearly zero power consumption and sub-picosecond latency [1-3]. However, the insufficient complexity of the network limits the scope of applications. Here, we demonstrate that the optical metasurface is used to construct an optical neural network for practically important and challenging medical image classification. The metasurface-based optical neural network is able to provide massive complex weights, whose number reaches an unprecedented scale of $\sim 10^7$ which conventional bulky optics cannot provide. Compared with state-of-art digital networks, we experimentally observed a remarkable reduction of network digital parameters ranging from $\sim 10^3$ to 10^5 times in a range of medical image classification tasks whilst maintaining comparable performance, as shown in Fig. 1.

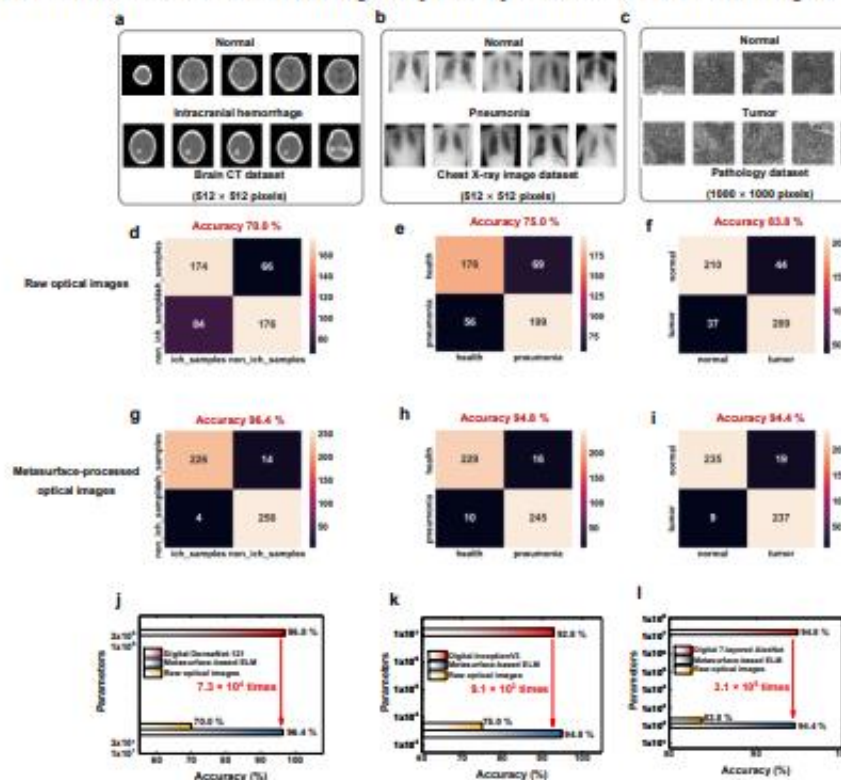


Fig. 1. (a), (b), (c) Three types of medical image datasets. (d), (e), (f) Classification accuracies obtained by the raw optical images. (g), (h), (i) Classification accuracies obtained by the metasurface-processed images. (j), (k), (l) The performance comparison with digital neural networks.

References

- [1] Zhou, Tiankuang, et al. "Large-scale neuromorphic optoelectronic computing with a reconfigurable diffractive processing unit." *Nat. Photonics* **15**, 367-373 (2021).
- [2] Luo, Xuhao, et al. "Metasurface-enabled on-chip multiplexed diffractive neural networks in the visible." *Light Sci. Appl.* **11**, 158 (2022).
- [3] Lin, Xing, et al. "All-optical machine learning using diffractive deep neural networks." *Science* **361**, 1004-1008 (2018).